Heliyon 10 (2024) e39933

Contents lists available at ScienceDirect

Heliyon

journal homepage: www.cell.com/heliyon

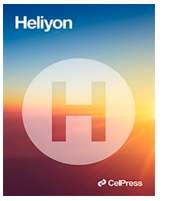

Research article

Structure-based virtual screening of natural compounds in preventing skin senescence: The role of epigallocatechin gallate in protein kinase C alpha-specific inhibition against UV-induced photoaging

Cheol Hyeon Cho [a,1], Woo-Jin Sim [a,1], Nam-Chul Cho [b], Wonchul Lim [c,**], Tae-Gyu Lim [a,c,*]

[a] Department of Food Science & Biotechnology, Sejong University, Seoul 05006, Republic of Korea
[b] Korea Chemical Bank, Korea Research Institute of Chemical Technology (KRICT), Daejeon, 34114, Republic of Korea
[c] Department of Food Science & Biotechnology, and Carbohydrate Bioproduct Research Center, Sejong University, Seoul 05006, Republic of Korea

ARTICLE INFO

Keywords:
Anti-skin aging
High-throughput screening
Human skin
Protein kinase C
Molecular docking

ABSTRACT

This study combines high-throughput screening and virtual molecular docking to identify natural compounds targeting PKC in skin aging. Go 6983, a PKC inhibitor, showed potent suppression of MMP-1 transcription. EGCG was one of the candidates that showed it could significantly lower UVB-induced MMP-1 expression in HaCaT cells, and it had a strong affinity for PKCα. Interestingly, EGCG is exclusively bound to PKCα, not the δ and ζ isoforms. Blocking PKCα did not elevate UVB-induced MMP-1 expression in HaCaT cells. In a model of human skin, EGCG stopped collagen breakdown and changes in epidermal thickness that were caused by UV light from the sun. This suggests that EGCG could be useful in dermatology and drug development. These findings highlight the role of structure-based screening in identifying candidate compounds with applications in the cosmetic, dermatological, preventive health, and pharmaceutical fields.

1. Introduction

The skin is the outermost organ covering our body, primarily consisting of the epidermis and dermis layers. As the outermost layer of the skin, the epidermis is mainly responsible for preventing damage from the external environment and determining skin color through pigmentation. As the lower layer of the epidermis, the dermis layer provides strength and elasticity to the skin with connective tissue and maintains hydration with hyaluronic acid [1,2]. Ultraviolet B (UVB) is one of the types of ultraviolet rays from the sun known to directly affect the epidermis of the skin, and prolonged exposure can lead to skin aging [3–5]. When the skin is exposed to UVB, the expression of matrix metalloproteinase-1 (MMP-1), also known as collagenase-1, increases in the epidermis layer. This enzyme promotes the breakdown of collagen fibers, the main structural protein in the skin, and contributes to the formation of wrinkles [6,7]. Collagen present in skin tissue plays an important role in providing tensile strength and elasticity to the skin, and during

* Corresponding author. Department of Food Science & Biotechnology, Sejong University, Seoul 05006, Republic of Korea.
** Corresponding author.
E-mail addresses: tglim@sejong.ac.kr (W. Lim), wlim@sejong.ac.kr (T.-G. Lim).
[1] These authors contributed equally to this paper.

https://doi.org/10.1016/j.heliyon.2024.e39933
Received 8 May 2024; Received in revised form 28 October 2024; Accepted 28 October 2024
Available online 30 October 2024

the photoaging process, the alignment of collagen fibers becomes irregular, making the skin appear aged [8].

Protein kinase C (PKC) is a key family of enzymes involved in signaling pathways that specifically phosphorylates substrates at serine and threonine residues, influencing a variety of cellular events such as cell proliferation and the regulation of gene expression [9,10]. A number of studies have emphasized that the activities of PKC are necessary for UVB-induced apoptosis of human keratinocytes and skin cell damage [11–13]. Different types of PKCs have different structures and substrate needs, which is why they are divided into three groups: "conventional" PKCs (cPKC), "novel" PKCs (nPKC), and "atypical" PKCs (aPKC). The cPKC family includes PKCα, PKCβ (PKCβI and PKCβII), and PKCγ. These proteins need calcium to work and are turned on by phosphatidylserine (PS) and the second messenger, diacylglycerol (DAG). nPKCs are made up of PKCδ, PKCε, PKCη, and PKCθ. They are controlled by PS and DAG and don't need calcium. The aPKC family, which includes PKCζ and PKCι (or PKCλ), operates without calcium and is controlled by PS. It doesn't need DAG to be activated [14–16]. Ongoing interest in the field of aging research endures, particularly concerning the significant role of PKC as implicated in the aging process, as highlighted in previous studies [17–19]. So, novel therapeutic agents for anti-skin aging induced by UVB need to be developed that only target certain PKC isoforms to prevent diseases associated with PKC [16].

Structure-based virtual screening (SBVS) models are currently recognized as crucial tools in the fields of life sciences and medicine. These models are utilized to analyze the molecular structures and interactions of compounds, aiding in the discovery of new bioactive substances [20]. Its high efficiency allows for rapid screening of extensive compound databases, facilitating the identification of promising molecules [21]. Additionally, its cost-effectiveness, compared to experimental methods, enables the evaluation of a diverse range of compounds at a relatively lower cost [22]. Moreover, SBVS provides the capability to visualize and interpret molecular interactions between compound structures and target proteins. However, SBVS comes with inherent limitations. The model's operation based on a single structure introduces the possibility of errors, susceptible to discrepancies with experimental data [21]. Furthermore, its scope may be limited to predicting the biological activity of specific molecules. Despite these difficulties, SBVS is still a useful tool for the search for novel bioactive compounds as seen in its use in the creation of therapeutic candidates for skin photoaging. Numerous studies have focused on drug discovery through SBVS. However, there aren't many structural biology studies that look into PKC-isoform-selective therapeutic agents using both methods at the same time.

In this study, we sought to identify an inhibitor to specifically suppress the PKC for mediating UVB-induced skin aging. The kinase inhibitor-based high-throughput system was used for specific kinases that were mainly responsible for contributing to anti-skin photoaging. We used SBVS models to discover novel PKC inhibitors in a library of natural compounds that were similar in three dimensions. The effect of natural inhibitor candidates on skin photoaging was validated in the human keratinocyte model HaCaT and the human skin tissue model.

2. Materials and methods

2.1. Reagents and antibodies

CellTiter 96® AQueous MTS Reagent Powder and reporter lysis 5 × buffer was obtained from Promega (Madison, WI, USA). Phenazine methosulfate, Go 6983 and active PKCα protein were purchased from Sigma-Aldrich (St. Louis, MO, USA). EGCG and polydatin were obtained from Selleckchem (Houston, TX, USA). Cyanidin chloride was purchased from Interpharm (Ilsandong-gu, Goyang-si, Republic of Korea). The CNBr-Activated Sepharose 4B bead was obtained from Cytiva (Marlborough, MA, USA). Myelin Basic Protein TFA was purchased from MedChemExpress (Monmouth Junction, NJ, USA). Antibodies against vinculin and MMP-1 were obtained from Santa Cruz Biotechnology (Dallas, TX, USA). Antibodies against PKC isoform antibody sampler kit and MMP-1 were purchased from Cell Signaling Technology (Danvers, MA, USA). MMP-1 luciferase reporter HaCaT cells and HaCaT cells (CLS Cell Lines Services GmbH, Germany, Catalog Number: 300493) were kindly provided by Prof. Ki Won Lee from Seoul National University. For authentication, these cells were verified through STR profiling and screened for mycoplasma contamination to confirm their purity and suitability for experimental applications.

2.2. Cell culture

Human keratinocyte HaCaT cells and MMP-1 luciferase reporter HaCaT cells were cultured in DMEM supplemented with 10 % FBS, 100 U/mL penicillin, and 100 μg/mL streptomycin. These cells were maintained at 37 °C under a 5 % CO_2 condition. MMP-1 luciferase reporter HaCaT cells were selected with 1 μg/mL of puromycin.

2.3. MMP-1 luciferase vector-transfected HaCaT

MMP-1 luciferase reporter HaCaT cells were cultured in 96-well plates at a density of 1.5×10^4 cells/well and maintained in Dulbecco's modified Eagle's medium (DMEM; Hyclone, Laboratories Inc, Logan, UT, USA) supplemented with 10 % (v/v) fetal bovine serum (FBS; Gibco, Waltham, MA, USA) and 1 % penicillin/streptomycin (Gibco). To induce experimental conditions, the cells underwent serum starvation for 24 h and were subsequently treated with various types of inhibitors (10 μM) for 1 h prior to exposure to UVB radiation. The UVB light source (Bio-Link Crosslinker; Vilber Lourmat, Marne-la-Vallee, France) emitted wavelengths of 254, 312, and 365 nm, with peak emission at 312 nm. After UVB exposure, the cells were incubated for an additional 5 h. After that, 20 μL of lysis buffer was added to break up the cells, and the luciferase activity was measured using the luciferase assay system (Promega, Madison, WI, USA) according to the manufacturer's instructions.

2.4. Molecular docking-based virtual screening

A molecular docking simulation was performed to virtually screen 20,969 natural compounds of the Korea Chemical Bank (KCB) using Schrodinger's program (Schrödinger, LLC, NY, USA). The PKCβII structure co-crystallized with a bisindolylmaleimide inhibitor (PDB code: 2I0E) was retrieved from the Research Collaboratory for Structural Bioinformatics (RCSB) database and employed as the receptor for the docking simulation. Structure was prepared with protonation at pH 7.4 and energy minimization. The grid for molecular docking with a 10 Å spacing around the kinase inhibitor in the ATP binding site, was generated. Natural compounds from the KCB chemical library were prepared using the Ligand structure preparation (LigPrep) module and subjected to docking using the Glide SP module. The virtual hits were ranked based on the glide score (G-score), and 64 compounds were selected for further biological evaluation through visual inspection. Then, three natural compound candidates were sorted for subsequent analysis.

2.5. MTS assay

To determine whether the impact of EGCG, polydatin, and cyanidin affects the viability of HaCaT cells, an MTS (3-(4,5-dimethylthhylthiazol-2-yl)-5-(3-carboxymethoxyphenyl)-2-(4-sulfophenyl)-2H-tetrazolium) assay was conducted. HaCaT cells were plated at a density of 1×10^5 cells/well in 96-well plates, followed by a 24 h serum starvation. Subsequently, the cells were treated with various concentrations (3.125, 6.25, 12.5, 25 and 50 μM) of EGCG, polydatin, and cyanidin. After incubation for 24 h, the cells were exposed to a 0.2 % (w/v) MTS solution containing phenazine methosulfate (PMS). The cells were then incubated at 37 °C in the dark for 1 h. After incubation for 1 h, the absorbance at 490 nm was measured using a microplate reader.

2.6. Western blotting analysis

HaCaT cells and human full-thickness skin tissue were washed with cold phosphate-buffered saline (PBS), permeated with 1 × cell lysis buffer for 10 min at 4 °C, and quantified with a Pierce BCA protein assay kit (Thermo Scientific, Waltham, MA, USA.). Equal amounts of protein were separated on 10 % sodium dodecyl sulfate-polyacrylamide gel electrophoresis (SDS-PAGE) at 110 V for 1 h and 40 min and transferred to a polyvinylidene difluoride (PVDF) membrane at 25 V for 15 min. Membranes were blocked with skim milk or a 5 % bovine serum albumin (BSA) solution for 1 h on a rack platform. The membranes were then incubated overnight with specific primary antibodies at 4 °C. After incubating, the membranes were washed three times with TBST for 10 min and incubated with the corresponding horse radish peroxidase-conjugated secondary antibodies for 40 min at room temperature. After washing the membrane, protein bands were detected using a chemiluminescence reader (LuminoGraph III Lite; ATTO, Tito-ku, Tokyo, Japan) at the Biopolymer Research Center for Advanced Materials, and protein expression was quantified using Image J software (National Institutes of Health, Bethesda, MD, USA).

2.7. Docking simulation of the PKC family and EGCG

The PKCα structure (PDB code: 3IW4) was obtained from the Protein Data Bank (PDB) and utilized as a template for homology modeling. Homology models of PKCδ and PKCζ, with amino acid sequence identities of 27 % and 29 %, respectively compared to the PKCα kinase domain, were generated based on the kinase domain of PKCα using the prime module of Schrodinger's software. Protein structures were prepared with protonation at pH 7.4 and subjected to energy minimization. The chemical structure of EGCG was retrieved from PubChem (PubChem CID: 65064), and its 3D structure was generated through energy minimization and protonation using LigPrep. The allosteric binding site of PKCα was supposed to be the most docked location of EGCG in the whole protein structure of PKCα using Autodock Vina software (La Jolla, CA, USA). EGCG was reattached to the allosteric binding sites of PKCα, PKCδ, and PKCζ using the Glide SP module. A low G-score was used to choose the binding pose.

2.8. Cell-based pull-down assays

Sepharose 4B powder (0.3 g) was reconstituted in a solution containing 1 mM HCl, and 2 mg EGCG was introduced into the coupling buffer (0.1 M $NaHCO_3$ and 0.5 M NaCl), followed by thorough mixing on a shaker at 4 °C overnight. The procedure was performed as reported in previous literature [23]. 500 μg of cellular protein extracted from HaCaT was incubated with either the EGCG-Sepharose 4B complex or Sepharose 4B alone beads at 4 °C overnight. The protein binding to the EGCG-Sepharose 4B complex was subsequently assessed by western blotting analysis.

2.9. Kinase activity assay

The *in vitro* PKCα kinase assay was executed employing the Universal Kinase Activity Kit (R&D Systems Inc., MN, USA). In brief, the PKCα kinase assay was performed using an active PKCα protein and initiated by adding the substrate mixture containing PKCα and the enzyme mixture containing myelin basic protein (MBP) or EGCG (0.5–2 μM) in a 96-well microplate, which was then incubated at 25 °C for 10 min. Subsequently, malachite green reagent was added to each well to terminate the reaction, followed by an additional incubation at 25 °C for 20 min. After incubation for 1 h, the absorbance at 620 nm was measured using a microplate reader.

2.10. Transfection with small interfering RNA

Scrambled small interfering RNA (siRNA) (sc-37007) and PKCα siRNA (sc-36243) were procured from Santa Cruz Biotechnology. Transient transfection of siRNA was conducted using the Lipofectamine™ CRISPRMAX™ Cas9 Transfection reagent (Thermo Scientific). Briefly, HaCaT cells were seeded at a density of 2×10^5 cells/well in 96-well plates and cultured until they attained 80 % confluence. HaCaT cells were treated with Lipofectamine and either scrambled siRNA or siPKCα (30 pmol) diluent using Opti-MEM™ (Gibco) in each well. After 5 h of incubation, the medium was replaced with complemented DMEM at 37 °C for 24 h. The western blotting analysis was used to see how well knockdown of the protein expression and Image J software (National Institutes of Health, Bethesda, MD, USA) to count the amount of protein expression.

2.11. Quantitative reverse transcription PCR (RT-qPCR)

HaCaT cells were seeded at a density of 3×10^5 cells in a 60 mm dish and incubated for 24 h. After 24 h of starvation, cells were treated with EGCG (0.5–2 μM). The cells were incubated for 1 h and cells were irradiated UVB. Total RNA was extracted from cells using TRIzol reagent (Thermo Fisher Scientific, MA, USA). Complementary DNA (cDNA) was synthesized from mRNA using the amfiRivert cDNA Synthesis Platinum Master Mix (GenDEPOT, Baker, TX, USA), according to the manufacturer's instructions. Briefly, the qRT- PCR was performed at 25 °C for 1 min, 51 °C for 30 min, and 85 °C for 1 min cDNA was mixed with primers and AccuPower® 2X GreenStar qRT-PCR MasterMix (GenDEPOT), and qRT-PCR was performed at 95 °C for 5 min, followed by 40 cycles at 95 °C for 15 s, 60 °C for 15 s, and 72 °C for 30 s. The MMP-1 forward primer sequence was 5′- CCC CAA AAG CGT GTG ACA -3′ and reverse primer sequence was 5′- GGT AGA AGG GAT TTG TGC G -3'. The GAPDH forward primer sequence was 5′- GTC TCC TCT GAC TTC AAC AGC -3′ and reverse primer sequence was 5′- GTC TCC TCT GAC TTC AAC AGC -3'.

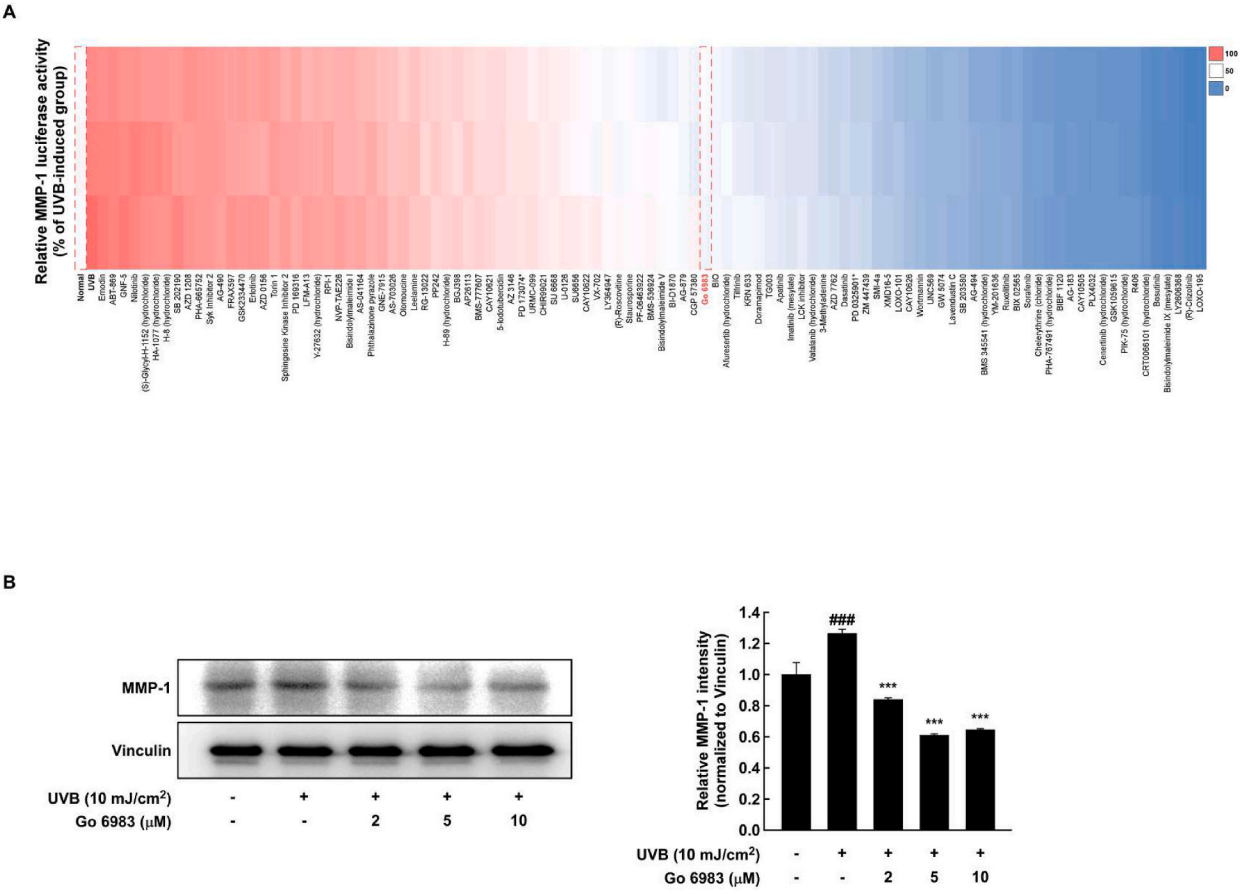

Fig. 1. Treatment of Go 6983 inhibited UVB-induced MMP-1 activation in the MMP-1-luc stable HaCaT cells. (**a**) Kinase inhibitor library for candidate suppressing UVB-induced MMP-1 transactivation by luciferase activity assay. (**b**) UVB-induced increased MMP-1 was assessed by Western blot and quantified with Image J software. $^{\#\#\#}p < 0.001$, $^{***}p < 0.001$.

2.12. Preparation of human skin tissue and solar UV irradiation

Abdominal human skin tissues were sourced from female Caucasian donors through Biopredic International (Rennes, France) in accordance with the French Law L.1245-2 CSP. Human skin provider, Biopredic International, holds approval from the French Ministry of Higher Education and Research for the acquisition, transformation, sale, and export of human biological material intended for research purposes (AC-2013-1754). This study adhered to all principles outlined in the Helsinki Declaration. Human skin tissues with a diameter of 10 mm were incubated in DMEM containing 10 % FBS with penicillin/streptomycin in a 5 % CO_2 incubator at 37 °C. *Ex vivo* human skin tissues were subjected to treatment with EGCG (0.0625–0.25 μM) and exposed to solar UV (25 kJ/m^2) radiation daily for a duration of 5 days (Fig. 5a).

2.13. Histological analysis

Fresh human full-thickness skin tissues were fixed with 4 % formaldehyde, embedded in paraffin, and then sectioned at appropriate intervals in three different locations. Subsequently, the sections were deparaffinized and utilized for subsequent experiments. For visualizing epidermal thickness, the Hematoxylin and Eosin staining kit (ab243880, Abcam, Cambridge, UK) was employed. Briefly, apply adequate Hematoxylin, Mayer's to completely cover tissue section and incubate for 5 min, washed two times with distilled water and then dipped in Bluing Reagent for 10 s. After two washes with distilled water, the tissue sections were dipped in ethanol and then

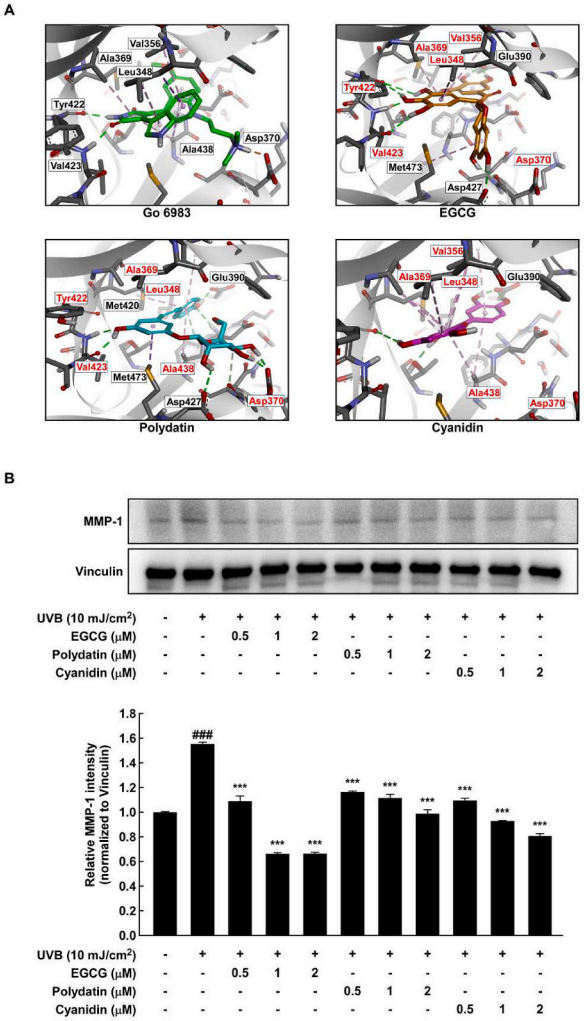

Fig. 2. Identification of common binding residues with Go 6983 in a natural compounds library SBVS: EGCG, polydatin, and cyanidin inhibit MMP-1 expression in HaCaT cells. (**a**) Natural product library SBVS a search was conducted to identify common binding residues with Go 6983, leading to the selection of EGCG, polydatin, and cyanidin. Red writing, common binding residues. (**b**) Cells were treated with candidate; EGCG, polydatin and cyanidin for 24 h. Protein expression of MMP-1 was determined by western blotting analysis and quantified with Image J software. $^{###}p < 0.001$, $^{***}p < 0.001$.

incubated in Eosin Y Solution for 2 min and then washed with pure alcohol. To visualize collagen fibers as a blue color, the Masson's trichrome staining kit (ab150686, Abcam, Cambridge, UK) was utilized. The tissues were initially placed in Bouin's Fluid preheated in a water bath at 64 °C, followed by storage in preheated Bouin's Fluid for 60 min and subsequent cooling for 10 min. Tissues were then sequentially stained with Weigert's Iron Hematoxylin, Biebrich Scarlet/Acid Fuchsin, Phosphomolybdic/Phosphotungstic Acid, and Aniline blue for 5–15 min each. Distilled water was used for washing between each staining step. Stained tissue slides were examined using an optical microscope. Epidermal thickness and the amount of collagen fibers were quantified using Image J software, respectively.

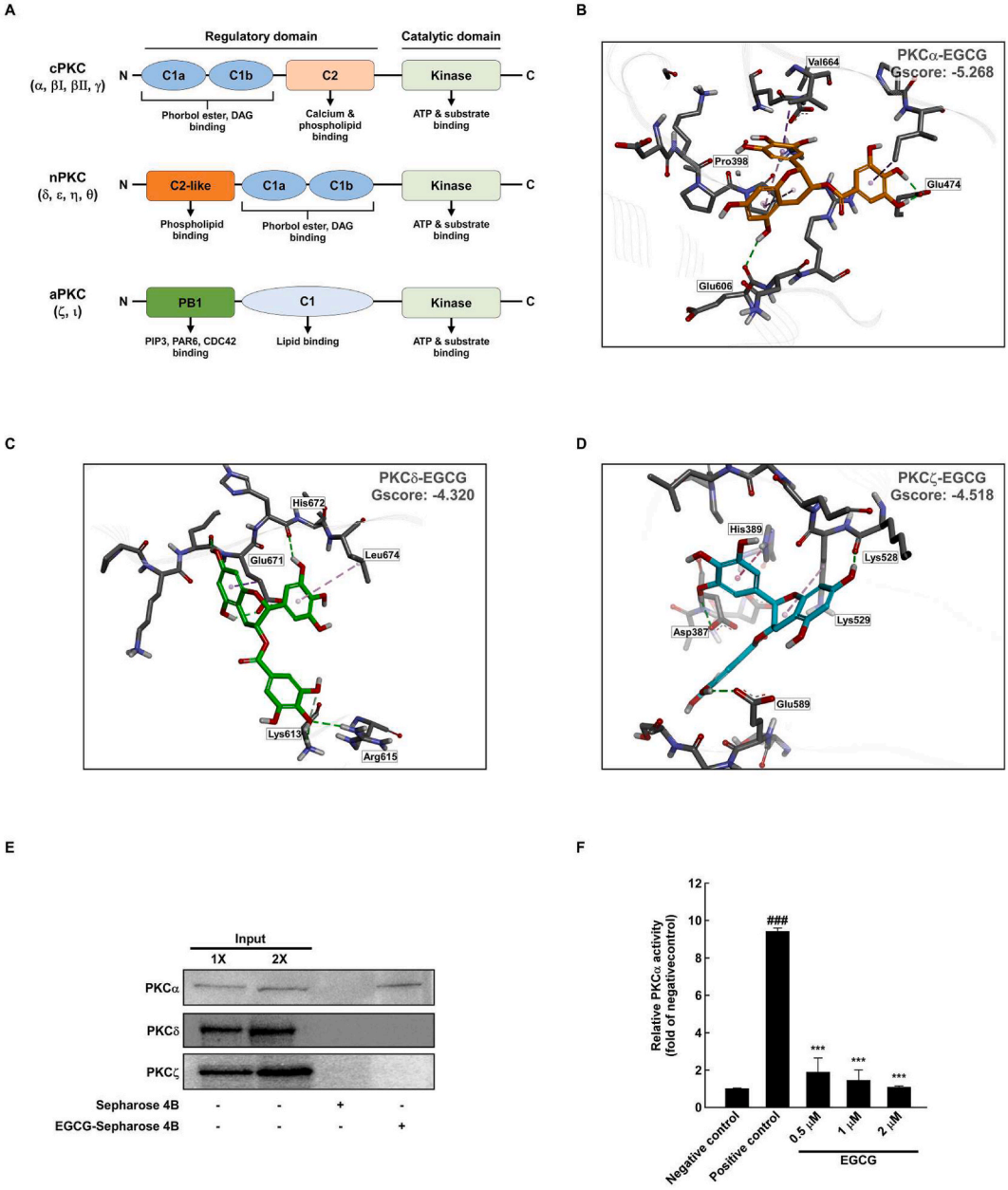

Fig. 3. *In silico* and *in vitro*, EGCG specifically inhibits PKCα by direct binding. (**a**) Classification and structural characteristics of protein kinase C family. (**b–d**) Binding affinity Gscore of the PKCα, PKCδ and PKCζ on EGCG. Binding affinities were measured by Schrodinger's software as described in the Materials and Methods. (**e**) EGCG directly binds to intracellular PKCα. The binding of EGCG with PKCα was performed SDS-PAGE and immunoblotting with a specific PKCα antibody: Lane 1, 2 (input control), cell lysates from HaCaT; Lane 3 (control), lysates from HaCaT; and Lane 4, cell lysates from HaCaT cells precipitated with EGCG-Sepharose 4B beads. (**f**) Effects of EGCG on PKCα kinase activity. Kinase activity was measured as described in the Materials and Methods. $^{###}p < 0.001$, $^{***}p < 0.001$.

2.14. Statistical analysis

Experimental data obtained from at least three independent experiments were presented as mean ± standard deviation. Statistical analysis was performed by one-way ANOVA with Tukey test or Student's t-test using GraphPad Prism software. Statistically significant differences were expressed as $^{\#\#}p < 0.01$ and $^{\#\#\#}p < 0.001$ compared to normal group; $^{**}p < 0.01$ and $^{***}p < 0.001$ compared to UVB-treated group.

3. Results

3.1. Go 6983 inhibits UVB-induced MMP-1 activation

To identify upstream regulators of MMP-1, a representative marker involved in skin aging caused by ultraviolet rays, a library of 192 kinase-specific inhibitors was treated with the MMP-1-luc stable HaCaT cell line, and the transactivation level of MMP-1 in the MMP-1-luc stable HaCaT cells was measured by a luciferase reporter gene assay. As shown in Fig. 1a, the transactivation of MMP-1 in UVB-irradiated cells was increased by about twofold compared to that of untreated control cells. It was found that 104 of the 192 kinase-specific inhibitors lowered the amount of MMP-1 transactivation that UVB caused. Not only that, but out of the 104 kinase-specific inhibitors, 94 notably decreased the level of MMP-1 transactivation by UVB ($p < 0.05$). Subsequently, 16 kinase inhibitors decreased the level of MMP-1 transactivation by UVB, similar to that of untreated cells. Interestingly, these inhibitors predominantly target PKC. Also, the PKC inhibitor Go 6983 significantly decreased the expression of MMP-1 protein stimulated by UVB in human keratinocyte HaCaT (Fig. 1b). These results reveal that PKC can be the target of UVB-irradiated skin aging.

3.2. Discovery natural compound candidates for anti-skin photoaging using computational docking stimulation

To discover natural compounds from the 20,969 candidates of the KCB database for development of PKC-specific inhibitor, the glide SP docking software was employed to rank-order compounds with protein-ligand binding affinity. In this study, we employed docking simulations with the co-crystallized structure of the cPKC member PKCβII isoform, along with a bisindolylmaleimide inhibitor exhibiting structural similarities to Go 6983. Virtual hits were sorted based on glide scores. Additionally, 64 compounds were compared with the amino acid residues of Go 6983 for biological evaluation, and then EGCG, polydatin, and cyanidin were sorted. Comparing EGCG, polydatin, and cyanidin with the amino acid residues bound to Go 6983, specific residues including Leu^{348}, Val^{356}, Ala^{369}, Asp^{370}, Tyr^{422}, Val^{423}, and Ala^{438} (highlighted in red) were identified (Fig. 2a). The MTS assay was used to test how harmful EGCG, polydatin, and cyanidin are to HaCaT cells. At concentrations below 3.125 μM, EGCG, polydatin, and cyanidin did not affect the growth of HaCaT cells (figs. S1a–c). When we exposed HaCaT cells to UVB light, we used Western blot analysis to see how the chemicals EGCG, polydatin and cyanidin changed the amount of MMP-1. As shown in Fig. 2b, these natural compound candidates

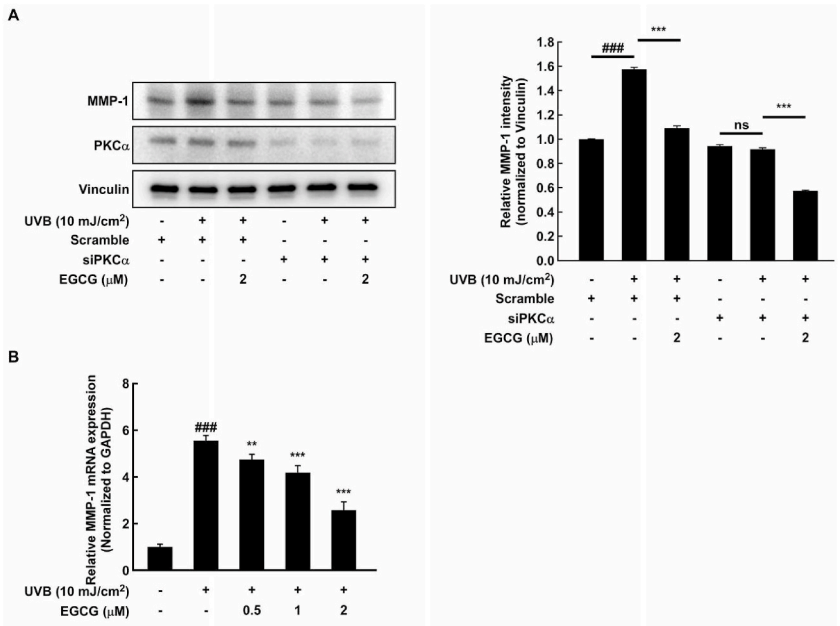

Fig. 4. Knockdown of PKCα inhibits UVB-induced MMP-1 expression. (**a**) In HaCaT cells, transfecting PKCα with siRNA resulted in a significant knockdown of PKCα protein expression and attenuated MMP-1 expression was determined by western blotting analysis and quantified with Image J software. (**b**) The mRNA levels of MMP-1 were detected using RT-qPCR. $^{###}p < 0.001$, $^{**}p < 0.01$, $^{***}p < 0.001$.

reduced UVB-induced MMP-1 expression. Furthermore, the reduction in MMP-1 expression by EGCG was significantly more pronounced compared to the treatment groups with polydatin and cyanidin.

3.3. EGCG is a specific natural inhibitor that directly binds to PKCα in silico and in vitro

PKC is classified into classical PKC, novel PKC, and atypical PKC according to subtype (Fig. 3a). Docking studies of EGCG with the structures of PKCα, PKCδ, and PKCζ gave us structural information about how EGCG binds to the PKC family. Most kinase activity is modulated through self-activating loop phosphorylation, leading to increased enzyme activity and altering the conformation of the loop. However, the interference of EGCG with PKC activity occurs because of its structural similarity to Go 6983, a known PKC

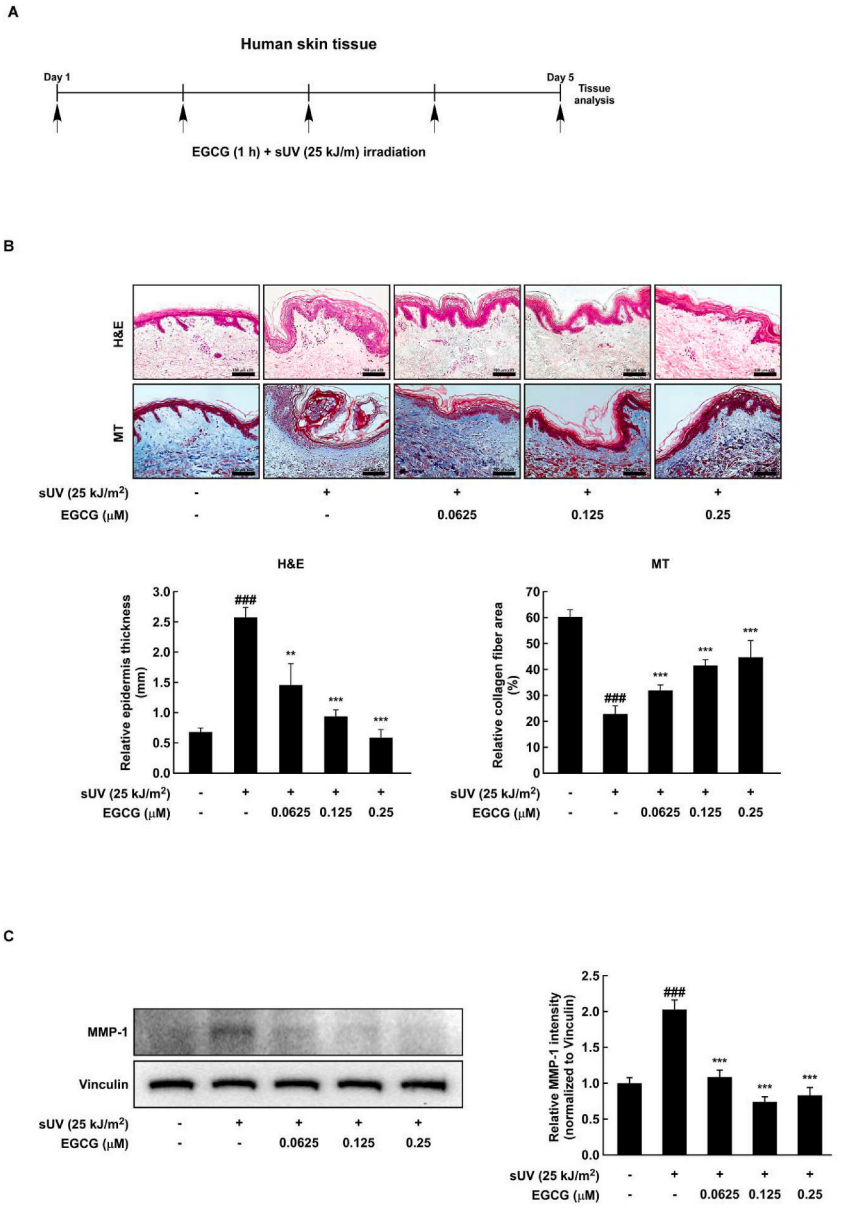

Fig. 5. EGCG prevents solar UV-induced MMP-1 expression, mitigating skin aging in *ex vivo* human skin tissue. (**a**) Human skin tissue samples were pre-treated with EGCG at the indicated concentrations for 1 h before being exposed to solar UV (25 kJ/m^2) over 5 days. Human skin tissues were subjected to solar UV at the same time each day. Human skin tissues from one Caucasian donor were used. (**b**) Epidermal thickness and collagen fibers were detected with H&E staining and Masson's trichrome staining, respectively. Human skin tissues were randomly divided into three sections (Black scale bars of the tissue image is 100 μm, respectively). H&E staining and Masson's trichrome staining were quantified using Image J software. $^{###}p < 0.001$, $^{**}p < 0.01$, $^{***}p < 0.001$. (**c**) MMP-1 and vinculin protein expression were determined in human skin tissue lysate by Western blot analysis and quantified using Image J software. $^{##}p < 0.01$, $^{***}p < 0.001$, $^{**}p < 0.01$.

inhibitor. Therefore, we assessed the Gscore, an indicator of binding affinity, by docking EGCG with the structures of PKCα, PKCδ, and PKCζ. A more negative Gscore corresponds to a higher binding affinity, with a difference of 1 value indicating a tenfold or greater disparity in binding affinity [24]. The obtained Gscore values were as follows: PKCα, −5.268; PKCδ, −4.320; and PKCζ, −4.520, indicating the highest binding affinity for PKCα (Fig. 3b–d). The molecular docking simulations between EGCG and PKCα showed the lowest Gscore compared to the other isoforms. This suggests that EGCG and PKCα have a very strong binding affinity. Therefore, we hypothesize that PKCα could potentially serve as a target for EGCG in regulating MMP-1 expression. We used EGCG and Sepharose 4B in HaCaT cell lysate in an *in vitro* pull-down assay to make sure it did interact directly with PKCα. These results showed that EGCG was directly and specifically bound to PKCα in the lysate from HaCaT cells (Fig. 3e). Since PKCα has been shown to turn on the MMP-1 pathway, we looked into whether there was a link between PKCα kinase activity and EGCG's ability to lower MMP-1. EGCG treatment decreased PKCα kinase activity in a way that depended on the dose, showing a significant reduction compared to the control group (Fig. 3f). Overall, we showed that EGCG stops UVB from increasing MMP-1 expression by directly stopping the activity of PKCα kinase. Additionally, this conclusion is supported by the observed direct binding of EGCG to PKCα protein in pull-down assays conducted on cell lysates.

3.4. PKCα plays a key role in UVB-induced MMP-1 expression in HaCaT cells

Because of the noticeable drop in PKCα kinase activity seen in my previous study with EGCG, we looked into the possible link between PKCα and UVB-induced MMP-1 expression in HaCaT cells by using siPKCα. When PKCα was turned off, MMP-1 expression did not go up compared to the controls that had their sequences jumbled (Fig. 4a). Additionally, EGCG suppressed UVB-induced MMP-1 expression in a concentration-dependent manner (Fig. 4b). Taken together, PKCα plays a key role in UVB-induced MMP-1 expression, and as a result, EGCG, which regulates PKCα activity, suppressed the gene expression of MMP-1.

3.5. EGCG prevents solar UV-induced photoaging in human skin tissue

In order to find out if EGCG could protect human skin tissues from changes in epidermal thickness and collagen fiber degradation caused by UV light, the tissues were treated with EGCG and exposed to UV light once a day for 5 days in a row (Fig. 5a). In this study, EGCG treatment demonstrated a decrease in the solar UV irradiation-induced thickening of the epidermal layer. Hematoxylin and eosin staining tests showed that EGCG treatment stopped the extra thickness of the epidermis that happens when human skin is exposed to solar UV light in dose-dependent manner. Furthermore, the EGCG-treated group exhibited an increased collagen fiber area in human skin tissues compared to the solar UV irradiation alone group. As shown by the Masson's trichrome staining assay, EGCG treatment prevented collagen fiber loss in human skin tissues after UV exposure in a way that depended on the dose (Fig. 5b). These findings demonstrate that EGCG's inhibitory effect on skin aging is evident not only in human skin cells but also in actual human skin tissues. MMP-1 induces skin aging by degrading collagen types I, respectively. We looked at how solar UV light affected the expression of MMP-1 in human skin specimens that had been treated with EGCG. Western blot analysis showed that the EGCG treatment efficiently blocked the expression of MMP-1 in human skin tissue lysate that was caused by UV light (Fig. 5c). Overall, exposure of human skin to solar UV radiation results in the degradation of collagen type I due to the upregulation of MMP-1, consequently leading to phenotypes such as wrinkles. Thus, EGCG is a potent anti-aging agent capable of normalizing MMP-1 expression levels.

4. Discussion

In response to the dynamic environmental changes, individuals strive to maintain a healthful lifestyle by employing pharmaceuticals, cosmetics, and dietary supplements [25,26]. The functional efficacy of these health-promoting products derives from their raw materials, aligning with the contemporary consumer preference for natural ingredient-based products [27]. Consequently, the identification of target molecules related to disorders and the discovery of natural candidates constitute essential stages in the development of health-promoting products [28–30]. In order to identify the crucial kinase responsible for UVB-induced skin aging, we screened the effect of a kinase inhibitor library on MMP-1 transactivation in this study. This study used structure-based 3D computer modeling to find natural anti-aging compounds that target UVB-irradiated skin before validating their effect on human skin tissues and cells.

HTS is a standard method for drug discovery in the pharmaceutical industry and is an approach to drug discovery that has grown in popularity over the past two decades. Advantages of this analysis system include cost savings and minimal space constraints. However, disadvantages include long design and implementation times, unstable operation, and limited error recovery capabilities [31].

UV-induced skin photoaging is well-known for its ability to induce MMP-1 overproduction, with MMP-1, recognized as a collagenase, playing a key role in degrading the ECM collagen fiber layer and contributing to skin sagging and wrinkle formation [3,32–34]. Although MMP-1, plays a role in skin aging, its involvement in ECM degradation across various physiological processes such as embryonic development, reproduction, and tissue remodeling led us to sort out the Go 6983 treated groups at levels similar to those of the normal groups [35,36]. Thus, Go 6983 was identified as a compound normalizing MMP-1 transcription, as illustrated in Fig. 1a and b, based on previous studies indicating that Go 6983, at concentrations up to 10 μM, does not affect viability [37].

SBVS, a computational approach in early-stage drug discovery that searches a chemical compound library for novel bioactive molecules against a specific drug target, integrates biophysics and computer science and is characterized by cost-effectiveness, speed, and flexibility of biophysical knowledge and algorithms related to molecular recognition [38]. It utilizes the 3D structure of the biological target, obtained from X-ray, NMR, or computational modeling, to dock compounds into the binding site and select a subset based on predicted binding scores for further biological evaluation [39]. Progress in molecular and structural biology has significantly

contributed to elucidating the 3D structure and function of various therapeutic biological molecules [40]. SBVS, emerging as a pivotal technique in the lead identification process, plays an important role and is presented as a complementary approach to HTS, enhancing the potential for lead identification when combined with structural biology [41,42]. Therefore, as shown in Fig. 2a, three natural compounds with structures similar to Go 6983 were chosen through SBVS.

As described in the introduction, PKC demonstrates a close association with the collagenase MMP-1. PKC translocates to various cellular regions in a stimulus-dependent manner and subtype, being implicated in various human diseases [43,44]. Nevertheless, the activity mechanisms for certain PKC subtypes remain unclear, requiring further investigation in future studies. Based on previous research showing that PKC is an MMP-1 upregulator [17–19], we hypothesized that three chosen Go 6983-like natural candidates would also possess inhibitory effects on PKC. As shown in Fig. 2b, UVB-induced MMP-1 overexpression in HaCaT cells was inhibited by three natural candidates, among which EGCG, known for its ability to downregulate signaling pathways mediated by reactive oxygen species [45], exhibited a particularly significant decrease.

EGCG, displaying the highest efficacy in inhibiting UVB-induced MMP-1 expression, belongs to the category of green tea polyphenols well-known for their anti-aging, neuroprotective, anti-inflammatory and properties [46–48]. Docking simulations were performed to investigate the association between EGCG and each PKC isoform, considering EGCG's role as a PKC inhibitor derived from natural products. As a result, EGCG exhibited binding to PKCα, PKCδ, and PKCζ isoforms; nevertheless, upon comparing the Gscore representing binding affinity [49], it demonstrated the highest affinity for PKCα (Fig. 3b–d). These findings demonstrate EGCG's function as a naturally sourced PKC inhibitor, particularly highlighting its potential as a PKCα-specific inhibitor. On the other hand, the variations in Gscore resulting from alters in the binding residues of EGCG to each PKC isoform necessitate further investigation.

The Gscore, reflecting the affinity between PKCα and EGCG, is recorded at −5.268, exhibiting a difference of approximately 1 compared to PKCδ and PKCζ. To verify EGCG's potential as a PKCα-specific inhibitor, an *in vitro* pull-down assay was performed between EGCG and various PKC isoforms. Consequently, EGCG bound to Sepharose 4B demonstrated its affinity towards PKCα in the HaCaT cell lysate (Fig. 3e). Following the *in vitro* pull-down assay, EGCG was confirmed for specific binding to PKCα. In addition, PKCα kinase activity was significantly decreased following EGCG application, indicating that the MMP-1 expression could be directly linked to PKCα kinase activity (Fig. 3f). Nevertheless, the results of docking simulations indicated a lower binding affinity towards PKCδ and PKCζ. This discrepancy is possibly due to the construction of homology models of PKCδ and PKCζ using the amino acid sequence identity from the PKCα domain, underscoring the need for additional structural biological studies. Moreover, the transfection of siRNA-PKCα neutralized the effect of EGCG on MMP-1 expression (Fig. 4a). In the PKCα knockdown group, UVB-induced MMP-1 overexpression was not observed; however, treatment with EGCG resulted in reduced MMP-1 expression, prompting the need for further validation regarding the potential downregulation of the PKCα sub-pathway by EGCG.

Finally, the phenotype was validated through *ex vivo* analysis using histological staining. Indications of skin aging include increased epidermal thickness combined with a reduce in the collagen fiber layer [50,51]. As shown in Fig. 5b, human skin tissues were analyzed for epidermal thickness and collagen fiber layer staining using H&E and Masson's trichrome methods. Solar UV irradiation of human skin tissue confirmed the expected degradation of the collagen fiber layer and subsequent increase in epidermal thickness, both of which were alleviated by EGCG treatment. Additionally, as shown in Fig. 5c, the overexpression of MMP-1 induced by solar UV irradiation was downregulated by EGCG treatment. However, the histological morphology was not clearly evident in this experiment, possibly due to the specimens being from elderly female Caucasian donors [52].

5. Conclusion

In summary, this study focuses on targeting skin photoaging by utilizing HTS and SBVS to identify potential natural compounds that inhibit MMP-1 expression. EGCG stands out as a prominent PKCα-specific inhibitor, effectively suppressing UVB-induced MMP-1 expression and preventing collagen degradation and changes in epidermal thickness induced by solar UV. These findings highlight the potential of structure-based systems for screening substances in diverse applications, including cosmetics, health supplements, and drug development.

CRediT authorship contribution statement

Cheol Hyeon Cho, Woo-Jin Sim and Nam-Chul Cho: performed the experiments and analyzed the data. Cheol Hyeon Cho, Nam-Chul Cho and Tae-Gyu Lim: conceived the project and contributed to the experimental design. Cheol Hyeon Cho, Woo-Jin Sim, Wonchul Lim and Tae-Gyu Lim: interpreted the results, prepared the figures, and wrote the original draft. Wonchul Lim and Tae-Gyu Lim: revised the manuscript.

Ethics statement

Human skin provider, Biopredic International, holds approval from the French Ministry of Higher Education and Research for the acquisition, transformation, sale, and export of human biological material intended for research purposes (AC-2013-1754).

Data availability

Data will be made available on request.

Declaration of competing interest

The authors declare that they have no known competing financial interests or personal relationships that could have appeared to influence the work reported in this paper.

Acknowledgments

This study was supported by the Ministry of Science and ICT and by the Bio & Medical Technology Development Program of the National Research Foundation (NRF) funded by the Ministry of Science & ICT (NRF-2022M3A9I5082349). And this research was supported by Basic Science Research Program through the National Research Foundation of Korea (NRF) funded by the Ministry of Education (2022R1A6A1A03055869 and RS-2023-00250405).

Appendix A. Supplementary data

Supplementary data to this article can be found online at https://doi.org/10.1016/j.heliyon.2024.e39933.

References

[1] S. Stander, et al., Cutaneous components leading to pruritus, pain, and neurosensitivity in atopic dermatitis: a narrative review, Dermatol. Ther. 14 (1) (2024) 45–57.
[2] J.H. Kim, Hyaluronic acid suppresses the effect of di-(2-ethylhexyl) phthalate in HaCaT keratinocytes, Molecular & Cellular Toxicology 18 (4) (2022) 549–556.
[3] Y. Liu, et al., Ferulic acid exhibits anti-inflammatory effects by inducing autophagy and blocking NLRP3 inflammasome activation, Molecular & Cellular Toxicology 18 (4) (2022) 509–519.
[4] C.H. Cho, et al., Oral administration of collagen peptide in SKH-1 mice suppress UVB-induced wrinkle and dehydration through MAPK and MAPKK signaling pathways, in vitro and in vivo evidence, Food Sci. Biotechnol. 33 (4) (2024) 955–967.
[5] S.J. Kim, et al., Network analysis to understand side effects of UVB on skin through transcriptomic approach, Molecular & Cellular Toxicology 18 (4) (2022), 647-647.
[6] S. Amano, Characterization and mechanisms of photoageing-related changes in skin. Damages of basement membrane and dermal structures, Exp. Dermatol. 25 (S3) (2016) 14–19.
[7] S. Wan, et al., Intestine epithelial cell-derived extracellular vesicles alleviate inflammation induced by Clostridioides difficile TcdB through the activity of TGF-beta1, Molecular & Cellular Toxicology (2022) 1–11.
[8] J.Y. Bae, et al., (-)Epigallocatechin gallate hampers collagen destruction and collagenase activation in ultraviolet-B-irradiated human dermal fibroblasts: involvement of mitogen-activated protein kinase, Food Chem. Toxicol. 46 (4) (2008) 1298–1307.
[9] I. Hamshaw, et al., The role of PKC and PKD in CXCL12 and CXCL13 directed malignant melanoma and acute monocytic leukemic cancer cell migration, Cell. Signal. 113 (2024) 110966.
[10] K.E. Lee, et al., Up-regulation of PKCα and δ during beating cardiomyocyte differentiation of P19CL6 cells with suppressed apoptotic cell populations, Molecular & Cellular Toxicology 20 (1) (2024) 167–176.
[11] H.J. Ko, et al., Ergothioneine alleviates senescence of fibroblasts induced by UVB damage of keratinocytes via activation of the Nrf2/HO-1 pathway and HSP70 in keratinocytes, Exp. Cell Res. 400 (1) (2021) 112516.
[12] B. Zhang, et al., Hydrogen ameliorates oxidative stress via PI3K-Akt signaling pathway in UVB-induced HaCaT cells, Int. J. Mol. Med. 41 (6) (2018) 3653–3661.
[13] R. Indirapriyadarshini, et al., Preventive effect of andrographolide against ultraviolet-B radiation-induced oxidative stress and apoptotic signaling in human dermal fibroblasts, Cell Biochem. Funct. 41 (8) (2023) 1370–1382.
[14] K.J. Way, E. Chou, G.L. King, Identification of PKC-isoform-specific biological actions using pharmacological approaches, Trends Pharmacol. Sci. 21 (5) (2000) 181–187.
[15] M. Spitaler, D.A. Cantrell, Protein kinase C and beyond, Nat. Immunol. 5 (8) (2004) 785–790.
[16] R. Garg, et al., Protein kinase C and cancer: what we know and what we do not, Oncogene 33 (45) (2014) 5225–5237.
[17] O. Bossi, et al., UV irradiation increases ROS production via PKCdelta signaling in primary murine fibroblasts, J. Cell. Biochem. 105 (1) (2008) 194–207.
[18] T.G. Lim, et al., The daidzein metabolite, 6,7,4'-Trihydroxyisoflavone, is a novel inhibitor of PKCalpha in suppressing solar UV-induced matrix metalloproteinase 1, Int. J. Mol. Sci. 15 (11) (2014) 21419–21432.
[19] R. Ricciarelli, et al., Age-dependent increase of collagenase expression can be reduced by alpha-tocopherol via protein kinase C inhibition, Free Radic. Biol. Med. 27 (7–8) (1999) 729–737.
[20] E.H.B. Maia, et al., Structure-based virtual screening: from classical to artificial intelligence, Front. Chem. 8 (2020) 343.
[21] E.H.B. Maia, et al., Molecular architect: a user-friendly workflow for virtual screening, ACS Omega 5 (12) (2020) 6628–6640.
[22] N.A. Murugan, et al., A review on parallel virtual screening softwares for high-performance computers, Pharmaceuticals 15 (1) (2022).
[23] S.K. Jung, et al., Myricetin suppresses UVB-induced skin cancer by targeting Fyn, Cancer Res. 68 (14) (2008) 6021–6029.
[24] A.J. Owoloye, et al., Molecular docking, simulation and binding free energy analysis of small molecules as PfHT1 inhibitors, PLoS One 17 (8) (2022) e0268269.
[25] A. Cencic, W. Chingwaru, The role of functional foods, nutraceuticals, and food supplements in intestinal health, Nutrients 2 (6) (2010) 611–625.
[26] A. Kassis, et al., Nutritional and lifestyle management of the aging journey: a narrative review, Front. Nutr. 9 (2022) 1087505.
[27] M. Siegrist, C. Hartmann, Consumer acceptance of novel food technologies, Nature Food 1 (6) (2020) 343–350.
[28] J.P. Hughes, et al., Principles of early drug discovery, Br. J. Pharmacol. 162 (6) (2011) 1239–1249.
[29] R.C. Mohs, N.H. Greig, Drug discovery and development: role of basic biological research, Alzheimer's Dementia 3 (4) (2017) 651–657.
[30] H.R. Kim, et al., Momordica charantia extracts obtained by ultrasound-assisted extraction inhibit the inflammatory pathways, Molecular & Cellular Toxicology 20 (1) (2024) 67–74.
[31] P. Szymanski, M. Markowicz, E. Mikiciuk-Olasik, Adaptation of high-throughput screening in drug discovery-toxicological screening tests, Int. J. Mol. Sci. 13 (1) (2012) 427–452.
[32] Y.C. Loo, et al., Development on potential skin anti-aging agents of Cosmos caudatus Kunth via inhibition of collagenase, MMP-1 and MMP-3 activities, Phytomedicine 110 (2023) 154643.
[33] P. Pittayapruek, et al., Role of matrix metalloproteinases in photoaging and photocarcinogenesis, Int. J. Mol. Sci. 17 (6) (2016).
[34] J.W. Shin, et al., Molecular mechanisms of dermal aging and antiaging approaches, Int. J. Mol. Sci. 20 (9) (2019).
[35] J.E. Fata, et al., Cellular turnover and extracellular matrix remodeling in female reproductive tissues: functions of metalloproteinases and their inhibitors, Cell. Mol. Life Sci. 57 (1) (2000) 77–95.

[36] M.F. Smith, et al., Ovarian tissue remodeling: role of matrix metalloproteinases and their inhibitors, Mol. Cell. Endocrinol. 191 (1) (2002) 45–56.
[37] Y.K. Park, B.C. Jang, UVB-induced anti-survival and pro-apoptotic effects on HaCaT human keratinocytes via caspase- and PKC-dependent downregulation of PKB, HIAP-1, Mcl-1, XIAP and ER stress, Int. J. Mol. Med. 33 (3) (2014) 695–702.
[38] M.H. Seifert, J. Kraus, B. Kramer, Virtual high-throughput screening of molecular databases, Curr. Opin. Drug Discov. Dev 10 (3) (2007) 298–307.
[39] Q. Li, S. Shah, Structure-based virtual screening, Methods Mol. Biol. 1558 (2017) 111–124.
[40] R.N. Dos Santos, L.G. Ferreira, A.D. Andricopulo, Practices in molecular docking and structure-based virtual screening, Methods Mol. Biol. 1762 (2018) 31–50.
[41] P.D. Lyne, Structure-based virtual screening: an overview, Drug Discov. Today 7 (20) (2002) 1047–1055.
[42] J. Vazquez, et al., Merging ligand-based and structure-based methods in drug discovery: an overview of combined virtual screening approaches, Molecules 25 (20) (2020).
[43] T.I. Igumenova, Dynamics and membrane interactions of protein kinase C, Biochemistry 54 (32) (2015) 4953–4968.
[44] T. Seki, et al., Phosphorylation of PKC activation loop plays an important role in receptor-mediated translocation of PKC, Gene Cell. 10 (3) (2005) 225–239.
[45] H. Tanabe, et al., Effects of epigallocatechin-3-gallate on matrix metalloproteinases in terms of its anticancer activity, Molecules 28 (2) (2023).
[46] Y. Jia, et al., (-)-Epigallocatechin-3-Gallate protects human skin fibroblasts from ultraviolet a induced photoaging, clinical, Cosmetic Investigational Dermatology 16 (2023) 149–159.
[47] J.E. Kim, M.H. Shin, J.H. Chung, Epigallocatechin-3-gallate prevents heat shock-induced MMP-1 expression by inhibiting AP-1 activity in human dermal fibroblasts, Arch. Dermatol. Res. 305 (7) (2013) 595–602.
[48] Y. Levites, et al., Involvement of protein kinase C activation and cell survival/cell cycle genes in green tea polyphenol (-)-epigallocatechin 3-gallate neuroprotective action, J. Biol. Chem. 277 (34) (2002) 30574–30580.
[49] C. Gueto-Tettay, et al., G-score: a function to solve the puzzle of modeling the protonation states of beta-secretase binding pocket, J. Mol. Graph. Model. 85 (2018) 1–12.
[50] B. Lynch, et al., A mechanistic view on the aging human skin through ex vivo layer-by-layer analysis of mechanics and microstructure of facial and mammary dermis, Sci. Rep. 12 (1) (2022) 849.
[51] S. Zhang, E. Duan, Fighting against skin aging: the way from bench to bedside, Cell Transplant. 27 (5) (2018) 729–738.
[52] Z. Zou, et al., A single-cell transcriptomic atlas of human skin aging, Dev. Cell 56 (3) (2021) 383–397 e8.